

these data were not enough to determine the structure of **1a**, X-ray analysis was performed on a mono-*p*-bromobenzoyl derivative (**1c**).¹⁰ The structure was determined by the direct method (MULTAN 78) and successive block-diagonal least-squares and Fourier synthesis. Parameters were refined by using anisotropic temperature factors to $R = 0.052$ for 1985 reflections [$|F_0| > 3\sigma(F_0)$]. Nineteen Bijvoet pairs which exhibited large effects of anomalous scattering from the bromine atoms were selected and used to determine the absolute configuration. All observed Bijvoet ratios were in agreement with the ones calculated for the chosen enantiomer in Figure 1. Consequently, phomactin A is (2*S*,3*S*,3*aS*,6*S*,7*R*,8*aR*)-3,3*a*-dihydroxy-2,6-(3'-methyl-3'-hexeno)-2,6,7-trimethyl-3*a*,5,6,7,8,8*a*-hexahydrofuro[2,3,4-*de*]chroman (**1a**). Some similar metabolites possessing a [9.3.1]pentadecane ring have been isolated from higher plants,¹¹ but this macrocyclic furochroman ring has not been found in natural products.

Phomactin A inhibited PAF-induced platelet aggregation (IC_{50} 1.0×10^{-5} M) and binding of PAF to its receptors (IC_{50} 2.3×10^{-6} M) but had no effect on adenosine diphosphate, arachidonic acid, and collagen-induced platelet aggregation. Thus, phomactin A is a new type of specific PAF antagonist. It is interesting that phomactin A has a glycerin-like subunit at C_2 , C_3 , and C_{3a} , since PAF itself has a glyceryl unit. This part may account for the activity. *Phoma* sp. produced many other phomactin derivatives, some of which were 10–100 times as active as **1a**. Structural analysis, derivatization, and structure-activity studies of these compounds are underway. Details will be reported elsewhere.

Acknowledgment. We thank Misses Y. Kuboniwa, T. Shimoji, and E. Yorikane of our laboratories for their technical assistance.

Supplementary Material Available: Experimental procedures and X-ray analysis data (16 pages). Ordering information is given on any current masthead page.

(10) **1c**: space group $P2_12_12_1$, $a = 9.239$ (1) Å, $b = 16.894$ (3) Å, $c = 15.900$ (2) Å, $V = 2481.8$ (5) Å³, $Z = 4$, $D_c = 1.38$ g/cm³, $\mu(\text{Cu K}\alpha) = 27.8$ cm⁻¹.

(11) (a) Burke, B. A.; Chan, W. R.; Honkan, V. A.; Blount, J. F.; Manchand, P. S. *Tetrahedron* **1980**, *36*, 3489–3493. (b) Karlsson, B.; Pilotti, A. M.; Söderholm, A. C.; Norin, T.; Sundin, S.; Sumimoto, M. *Tetrahedron* **1978**, *34*, 2349–2354.

Bifunctional Monomolecular Langmuir–Blodgett Films at Electrodes. Electrochemistry at Single Molecule “Gate Sites”

Renata Bilewicz[†] and Marcin Majda*

Department of Chemistry
University of California in Berkeley
Berkeley, California 94720

Received April 3, 1991

Control of reactivity at the electrode/solution interface through control of chemical and structural features of interfacial films has been a major goal in electrochemistry.¹ Below, we describe a monomolecular surface assembly of long chain amphiphilic molecules which allows us to channel access to the electrode surface through a controlled number of single molecule “gate sites”. The monolayer assembly is bifunctional in its structure and properties and consists of two types of molecules, those that passivate the electrode and those which open access to its surface. Octadecanethiol ($C_{18}SH$) and octadecyl hydroxide ($C_{18}OH$) are used together to block access to the electrode.² Ubiquinone (Q_{10}),

[†] Permanent address: Department of Chemistry, Warsaw University, Pasteura 1, 02-093 Warsaw, Poland.

(1) Fujihira, M. In *Topics in Organic Electrochemistry*; Fry, A. J., Britton, W. E., Eds.; Plenum Publishing Corp.: New York, 1986; Chapter 6, p 255.
(2) Bilewicz, R.; Majda, M. *Langmuir*. Submitted for publication.

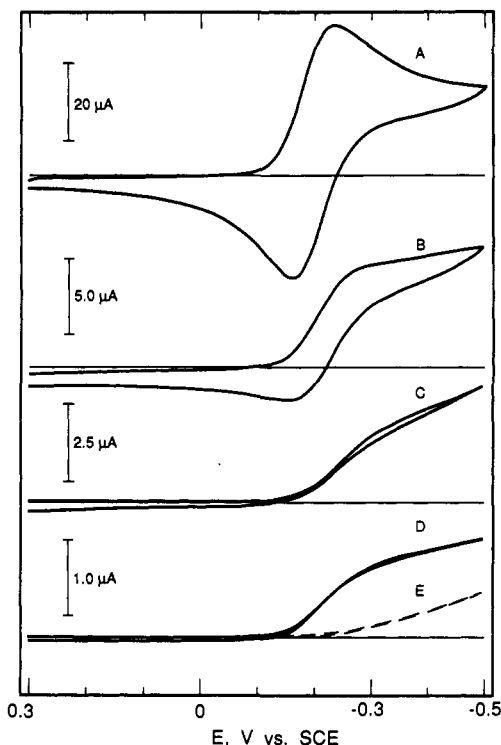
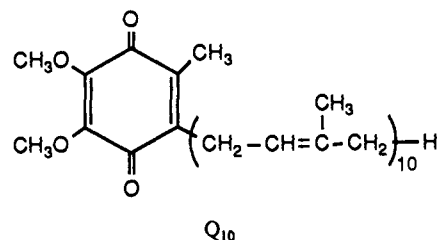


Figure 1. Cyclic voltammograms of $Ru(NH_3)_6^{3+}$ (1.0 mM in 0.5 M KCl) at a bare gold electrode (A) and those coated with $Q_{10}/C_{18}SH/C_{18}OH$ L-B monolayers ($X_{C_{18}SH}:X_{C_{18}OH} = 2.3$, L-B transfer pressure, 20 mN/m). Surface concentrations of Q_{10} (in mol/cm²): B, 2.5×10^{-15} ; C, 5.4×10^{-17} ; D, 1.9×10^{-17} ; E, 0. $A = 0.40$ cm², $v = 50$ mV/s.

a long-chain benzoquinone derivative shown below, acts as a gate site. The monolayer film is initially assembled at the air/water



interface where it is compressed and then deposited at the electrode surface by the Langmuir–Blodgett (L–B) method.²

Formation of monolayers of long-chain surfactants on solid surfaces can be accomplished by the L–B method or via spontaneous self-assembly.³ Densely packed self-assembled alkyl thiol monolayers were investigated as model organic surfaces⁴ and used in the studies of long-range electron-transfer kinetics,⁵ where compact alkyl thiol layers provided tunneling barrier of adjustable thickness.⁶ Coassembly of octadecanethiol and a nonamphiphilic component on gold electrodes led to the formation of surface assemblies with ion-selective⁷ or catalytic properties.⁸ In comparison with self-assembly, L–B techniques offer two important advantages. One is a broader range of applications, since one is not limited to thiol derivatives. The other is precise control of composition of mixed monolayer assemblies. We showed recently that monomolecular L–B films consisting of ca. 70 mol% of $C_{18}SH$

(3) For a review of recent literature, see, for example: Whitesides, G. M.; Laibinis, P. E. *Langmuir* **1990**, *6*, 87.

(4) Bain, C. D.; Whitesides, G. M. *Angew. Chem., Int. Ed. Engl.* **1989**, *28*, 506.

(5) Chidsey, C. E. D. *Science* **1991**, *251*, 919.

(6) Miller, C.; Cuendet, P.; Gratzel, M. *J. Phys. Chem.* **1991**, *95*, 877.

(7) Rubinstein, I.; Steinberg, S.; Tor, Y.; Shanzer, A.; Sagiv, J. *Nature* **1988**, *332*, 426.

(8) Kunitake, M.; Akiyoshi, K.; Kawatana, K.; Nakashima, N.; Manabe, O. *J. Electroanal. Chem.* **1990**, *292*, 277.

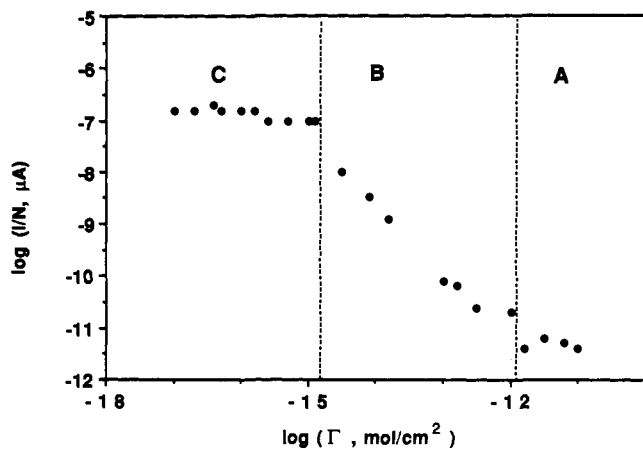


Figure 2. Plot of $\text{Ru}(\text{NH}_3)_6^{3+}$ limiting reduction current per Q_{10} site vs Q_{10} surface concentration.¹¹ The increase in i/N reflects mass-transport enhancement due to radial diffusion to the individual Q_{10} sites (see text). Experimental conditions are described in Figure 1.

and 30 mol% of C_{18}OH can be transferred onto gold-coated glass substrates at ca. 20 mN/m and that their passivating properties and stability are essentially identical with the best examples of self-assembled C_{18}SH films known in the literature.²

In the experiments described below, mixed $\text{C}_{18}\text{SH}/\text{C}_{18}\text{OH}$ L-B monolayers provide a means of immobilization of ubiquinone at a controlled surface concentration at the electrode surface. We discovered that incorporation of Q_{10} into a passivating $\text{C}_{18}\text{SH}/\text{C}_{18}\text{OH}$ L-B monolayer removes its passivating character and allows electroactivity of the $\text{Ru}(\text{NH}_3)_6^{3+/2+}$ couple. Consider the cyclic voltammograms in Figure 1. As the mole fraction of Q_{10} in the L-B film decreases,⁹ the shape of the voltammograms becomes sigmoidal, suggesting increasing contribution of spherical diffusion. Ultimately, the plateau current of $\text{Ru}(\text{NH}_3)_6^{3+}$ reduction in Figure 1D becomes independent of the voltammetric scan rate (20–1000 mV/s). These results are consistent with the reduction taking place at the individual Q_{10} sites in the otherwise passivating $\text{C}_{18}\text{SH}/\text{C}_{18}\text{OH}$ monolayer. As the site density decreases, hemispherical diffusion zones formed around individual Q_{10} gate sites cease to overlap on the time scale of these experiments. This model implies that the mass-transport rate to the individual Q_{10} centers (and thus reduction current) increases as their surface density decreases.¹⁰ This is indeed observed, as shown in Figure 2, where the current per Q_{10} site¹¹ is plotted vs their surface concentration. The three regions in Figure 2 correspond to linear diffusion (A), mixed linear and radial diffusion (B), and hemispherical diffusion (C). In the latter case, the magnitude of i/N , where N is the number of Q_{10} molecules at the electrode surface,⁹ is in good agreement with the expression for current at a microdisk electrode with radius r ¹²

$$i = 4nFrDC^* \quad (1)$$

where D and C^* are the diffusion coefficient and bulk concentration of $\text{Ru}(\text{NH}_3)_6^{3+}$. Assuming $r = 5 \text{ \AA}$,¹³ one obtains $i = 9.7 \times 10^{-14} \text{ A}$ from eq 1. The average current per Q_{10} site observed experimentally in region C of Figure 2 is $1.5 \pm 0.3 \times 10^{-13} \text{ A/molecule}$ (based on over 20 independent experiments).

A mathematical description of nonlinear diffusion effects at arrays of microelectrodes was presented recently by Amatore and

Table I. Comparison of the Observed and Calculated Current Values Due to Reduction of $\text{Ru}(\text{NH}_3)_6^{3+}$ at Au Electrodes Coated with $Q_{10}/\text{C}_{18}\text{SH}/\text{C}_{18}\text{OH}$ L-B Monolayers^a

$\Gamma_{Q_{10}} \times 10^{16}$ mol/cm ²	i_{obs}^b μA/cm ²	i_{calc}^c μA/cm ²
0.19	1.9 ± 0.5	1.6
0.38	4.0 ± 0.6	3.2
1.68	15.7 ± 1.1	14.1
2.35	18.2 ± 2.7	19.7

^a Experimental conditions are given in Figure 1. ^b The average current values were obtained based on experiments with 3–6 electrodes each. ^c Calculated based on eqs 2 and 3.

co-workers.¹⁰ For the case corresponding to the experimental conditions in region C of Figure 2, they derived the following expression for the total current to the array of hexagonally distributed, widely spaced microdisk electrodes

$$i = nFAC^*D(1 - \theta)^{1/2}/0.6R_0 \quad (2)$$

$$(1 - \theta)^{1/2} = R_a/R_0 \quad (3)$$

where A is the total electrode surface area, θ is fractional coverage of a passivating film, R_a is a radius of an individual active site,¹³ and R_0 is half of the distance between adjacent active sites.¹⁴ On the basis of these equations, and assuming again $R_a = 5 \text{ \AA}$, we obtained the current values in agreement with the experimental results in region C of Figure 2 as shown in Table I. This agreement substantiates the notion that individual ubiquinone molecules act as gate sites in controlling access of $\text{Ru}(\text{NH}_3)_6^{3+}$ to the electrode surface. It is worth noting that the strength of this argument is based on the agreement between the experiment and the theoretical model involving both the number of Q_{10} sites and their radius.

In view of these data, it appears that the isoprenoid chain of ubiquinone forms a channel which spans the thickness of the $\text{C}_{18}\text{SH}/\text{C}_{18}\text{OH}$ monolayer and provides a "gate" of sufficiently large diameter to allow $\text{Ru}(\text{NH}_3)_6^{3+}$ to approach the electrode surface (cross-sectional areas of Q_{10} ¹³ and $\text{Ru}(\text{NH}_3)_6^{3+}$ ¹⁵ are ca. 85 and 41 \AA^2 , respectively). An unhindered access of $\text{Ru}(\text{NH}_3)_6^{3+}$ to the electrode surface implied in this model is further supported by a large apparent heterogeneous rate constant of $\text{Ru}(\text{NH}_3)_6^{3+}$ reduction which can be obtained from a shift of the half-wave potential, $E_{1/2}$, relative to the formal potential, E° , measured at a clean gold electrode (see Figure 1 (parts A and D)). The following equation derived by Amatore et al. can be used¹⁰

$$k_{\text{app}} = (D/0.6R_a) \exp[(\alpha F/RT)(E_{1/2} - E^\circ)] \quad (4)$$

The average value of the measured shift of $-38 \pm 1 \text{ mV}$ (based on 10 independent experiments) leads to the k_{app} of $79 \pm 1.3 \text{ cm/s}$. It is important to point out that the reduction of the ruthenium complex is not mediated by the quinone moiety of Q_{10} since its reduction potential in 0.5 M KCl is -0.41 V vs SCE . Recently, Penner et al. obtained an equally high value of the heterogeneous rate constant for this redox couple of $79 \pm 44 \text{ cm/s}$ under the same conditions on underivatized 10- \AA radius Pt "nanodes".¹⁶ The role of the quinone group, Cl^- ions, and possible migration effects on the value of the apparent rate constant in our experiment are subjects of current investigations.

The ability to channel access to the electrode surface through single molecule gate sites, which we demonstrated here, opens new possibilities of designing monolayer assemblies in which chemical structure of the gate molecules could be used to induce elements

(9) We assume that Q_{10} concentration at the electrode surface is equal to its value at the water surface in the corresponding L-B transfer experiment. A 1:1 correlation of Q_{10} surface concentration at the air/water interface and at the electrode surface following L-B transfer was demonstrated electrochemically² in the concentration range 1.0×10^{-12} – $1.0 \times 10^{-10} \text{ mol/cm}^2$.

(10) Amatore, C.; Savéant, J.-M.; Tessier, D. *J. Electroanal. Chem.* **1983**, *147*, 39.

(11) Voltammetric peak currents (at 50 mV/s) were measured in region A and in part of region B, while plateau currents were measured at lower Q_{10} concentrations where sigmoidal voltammograms were obtained.

(12) Howell, J. O.; Wightman, R. M. *Anal. Chem.* **1984**, *56*, 524.

(13) The radius of a Q_{10} site was obtained from the cross-sectional area of Q_{10} in a $\text{C}_{18}\text{SH}/\text{C}_{18}\text{OH}$ monolayer at the air/water interface of $84.6 \pm 0.5 \text{ \AA}^2/\text{molecule}$.

(14) R_0 values were calculated from the known Q_{10} surface concentrations at the air/water interface.

(15) Sutin, N.; Brunswig, B. S.; Creutz, C.; Winkler, J. R. *Pure Appl. Chem.* **1988**, *60*, 1817.

(16) Penner, R. M.; Heben, M. J.; Longin, T. L.; Lewis, N. S. *Science* **1990**, *250*, 1118.

of molecular recognition and selectivity in electrochemical reactions.

Acknowledgment is made to the donors of the Petroleum Research Fund, administered by the American Chemical Society, for partial support of this research. We also acknowledge and thank the National Science Foundation for supporting this research under Grant CHE-8807846.

Conformational Selectivity in Molecular Recognition: The Influence of Artificial Receptors on the Cis-Trans Isomerization of Acylprolines

Cristina Vicent, Simon C. Hirst, Fernando Garcia-Tellado,[†] and Andrew D. Hamilton*

Department of Chemistry, University of Pittsburgh
Pittsburgh, Pennsylvania 15260

Received February 25, 1991

The cis-trans isomerization of acylprolyl groups (Figure 1) is a kinetically significant step in protein folding¹ and, as such, has been the subject of intense scrutiny.² This interest has increased with the recent identification of a family of enzymes that catalyze this interconversion and the important role that two of their number, cyclophilin³ and FK506 binding protein,⁴ play in immunosuppression. The peptidyl prolyl isomerases (PPIases) have been investigated by spectroscopic,^{5,6} synthetic,⁶ and kinetic⁷ methods, and a catalytic mechanism involving amide-bond distortion has been proposed. Our interest lay in modeling this process, and we report herein that different synthetic receptors can discriminate between the two rotamers and so influence the acylproline s-cis-s-trans equilibrium.

In most acylprolines the s-trans rotamer is favored over the s-cis due to the steric demands of the acyl group.^{2c} In succinamide diacid **1**^{8,9} the s-cis:s-trans ratio is approximately 1:3.5. During this equilibrium the carboxylic acid groups move from 6.9 Å apart in s-trans-**1b** to 5.5 Å apart in s-cis-**1a**.¹¹ This suggested that an artificial receptor with appropriately spaced carboxylic acid binding groups might selectively complex s-cis-**1a** and so shift the equilibrium toward the less favorable rotamer. We have previously established¹² that terephthaloyl receptor **2** (NH-NH distance, 7.32 Å) binds strongly to aliphatic dicarboxylic acids (as in Figure 2). Molecular mechanics calculations¹¹ showed that **2** is well-suited to bind selectively to s-cis-**1a** compared to s-trans-**1b** (Figure 3). Addition of 1 equiv of **1** to a CDCl₃ solution of **2** resulted

[†] On leave from Instituto de Productos Naturales Organicos del CSIC, Tenerife, Spain.

(1) Brandts, J. F.; Halvorson, H. R.; Brennan, M. *Biochemistry* **1975**, *14*, 4953. Fischer, G.; Schmid, F. X. *Biochemistry* **1990**, *29*, 2205.

(2) (a) Grathwohl, C.; Wüthrich, K. *Biopolymers* **1976**, *15*, 2025. (b) Hetzel, R.; Wüthrich, K. *Biopolymers* **1979**, *18*, 2589. (c) Nishihara, H.; Nishihara, K.; Uefuji, T.; Sakota, N. *Bull. Chem. Soc. Jpn.* **1975**, *48*, 553.

(3) Takahashi, N.; Hayano, T.; Suzuki, M. *Nature* **1989**, *337*, 473. Fischer, G.; Wittmann-Liebold, B.; Lang, K.; Kiefhaber, T.; Schmid, F. X. *Nature* **1989**, *337*, 476.

(4) Harding, M. W.; Galat, A.; Uehling, D. E.; Schreiber, S. L. *Nature* **1989**, *341*, 758.

(5) Hsu, V. L.; Handschumacher, R. E.; Armitage, I. M. *J. Am. Chem. Soc.* **1990**, *112*, 6745.

(6) Nakatsuka, M.; Ragan, J. A.; Sammakia, T.; Smith, D. B.; Uehling, D. E.; Schreiber, S. L. *J. Am. Chem. Soc.* **1990**, *112*, 5583.

(7) (a) Harrison, R. K.; Stein, R. L. *Biochemistry* **1990**, *29*, 1684. (b) Albers, M. W.; Walsh, C. T.; Schreiber, S. L. *J. Org. Chem.* **1990**, *55*, 4984.

(8) Formed from proline and succinic anhydride.

(9) Proline diacids of type **1** are interesting both as derivatives of AspPro and as ACE inhibitors¹⁰ related to captopril and enalapril.

(10) Rich, D. H. *Comprehensive Medicinal Chemistry*; Sammes, P. G., Taylor, J. B., Eds.; Pergamon Press: Oxford, 1990; Vol. 2, p 404.

(11) Using MacroModel v.2. Still, W. C. Columbia University.

(12) Garcia-Tellado, F.; Goswami, S.; Chang, S. K.; Geib, S. J.; Hamilton, A. D. *J. Am. Chem. Soc.* **1990**, *112*, 7393.

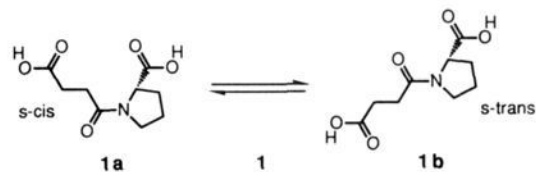


Figure 1.

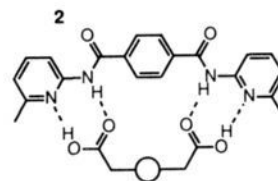


Figure 2.

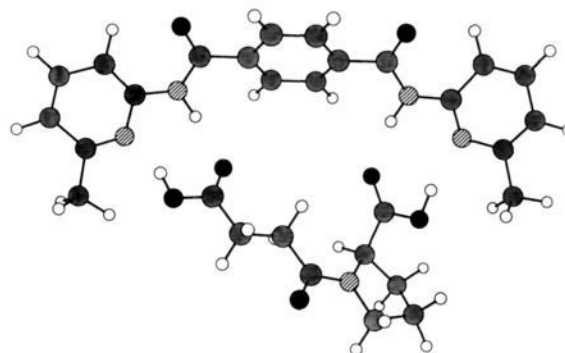


Figure 3.

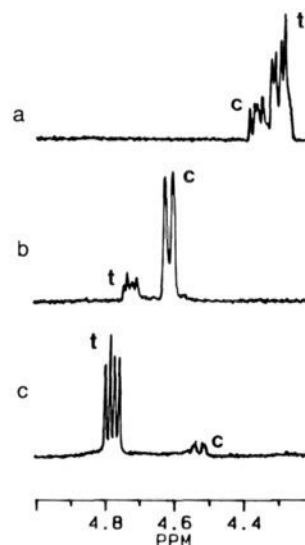


Figure 4. The proline α H region of the ¹H NMR spectra of (a) proline fumaramide **3**,^{15a} (b) a 1:1 mixture of **2** and **3**,^{15b} and (c) a 1:1 mixture of **6** and **3**.^{15b}

in a change in the s-cis:s-trans ratio to 3:2.¹³ That this selective stabilization is due to binding is seen by the large downfield shifts (from 8.5 to 11.1 ppm)¹² of the amide NH resonances of **2**, as expected for the formation of a tetra-hydrogen-bonded complex of the type shown in Figure 3. Also, a downfield shift (0.4 ppm) of the succinamide α CH₂ confirms the position of the substrate within the cavity. The small preference shown by **2** for s-cis-**1a** may be due to the flexibility of the succinamide chain which, when

(13) Rotamer ratios were measured by integration of proline α H signals in the ¹H NMR spectra, and assignments were made by ¹³C NMR shift comparisons.¹⁴

(14) Dorman, D. E.; Bovey, F. A. *J. Org. Chem.* **1973**, *38*, 2379.